Simultaneous resource recovery and ammonia volatilization minimization in animal husbandry and agriculture

M. Ganesapillai [a],*, Prithvi Simha [b,c], Karan Desai [a], Yash Sharma [a], Tabrez Ahmed [a]

[a] *Mass Transfer Group, Department of Chemical Engineering, VIT University, Vellore 632014, Tamil Nadu, India*
[b] *School of Earth, Atmospheric and Environmental Sciences (SEAES), The University of Manchester, Oxford Road, Manchester M13 9PL, United Kingdom*
[c] *Department of Environmental Sciences and Policy, Central European University, Nádor utca 9, 1051 Budapest, Hungary*

Abstract

The study demonstrates that the minimization of ammonia volatilization and urea recovery could be coupled through the use of physical adsorption processes in continuous packed-bed columns. The potential of using microwave activated coconut shell based activated carbon toward the recovery of urea from cattle urine was investigated. The prepared carbon was immobilized onto etched glass beads to investigate the effect of initial concentration, flow rate and size of carbon support in a continuous, down-flow mode packed column. Further, to describe the sorption behavior, the experimental data were tested against different kinetic models. The analysis of the breakthrough curves allowed identification of the favorable operating parameters as: sorbate flow (8 L·h^{-1}), initial urea concentration (60%) and glass bead support size (ϕ 1.5 cm). An equilibrium sorption of 802.8 mg·g^{-1} and up to 80% urea recovery was observed. Regeneration studies allowed for nearly 95% urea recovery with sorbent capacity decreasing by 5% over seven cycles of sorption/desorption.

1. Introduction

It has long been recognized that there are certain physical limits on the global availability of economically-valuable natural resources underlying their potential exhaustibility [1]. However, for effective stewardship of earth's resources, it is evident that the economy–environment interaction must acknowledge these ecological constraints. Despite this understanding, our industrial activities seem to operate contrary to what is required for them to be sustainable. This phenomenon is clearly evident in the procurement of minerals and resources by the fertilizer industry which has tripled its output since the 1960s [2]. While technological modernization of agriculture has allowed its intensification commensurate with synthetic fertilizer use bringing the obvious benefits of increased food production, the ecological degradation accompanying this has been extensive and well-documented [3–5]. On the other hand, sustainability, a human construct, has seen its comprehension and applicability to various circumstances evolves continuously over time. Sustainability in agricultural production systems is now being seen through the lens of resource recovery where enhancing crop productivity through resources recovered from wastes is seen as a potential solution to ensure food security [6–9].

Cattle urine is one such resource where nutrient recovery would be beneficial. Feedlot cattle is known to retain less than 20% of dietary nitrogen (N) indicating that more than 80% of it finds its way in cattle excreta [10]. Although 60–80% of this N is excreted as urine, it undergoes rapid conversion thereafter to result in ammonia volatilization. This loss of ammonia to the environment contributes to its increased atmospheric concentration as ammonium sulfate ($(NH_4)_2SO_4$), ammonium nitrate (NH_4NO_3) and ammonium chloride (NH_4Cl) that are subsequently removed by dry and/or wet acid deposition [11]. Atmospheric mobilization and deposition of NH_3 have disturbed the nutrient balance of natural ecosystems [12], induced acute toxicity and secondary metabolic changes in vegetation [13], and

_____

* Corresponding author. Department of Chemical Engineering, VIT University, Vellore 632014, India. Tel.: +91 97902 99447; fax: +91 416 224 3092.

E-mail addresses: drmaheshgpillai@gmail.com; maheshgpillai@vit.ac.in (M. Ganesapillai).

Nomenclature

A	Area under break through curve [m^2]
C_{ads}	Adsorbed urea concentration [g·L^{-1}]
C_b	Breakthrough concentration [mg·L^{-1}]
C_o	Inlet sorbate concentration [g·L^{-1}]
C_t	Outlet sorbate concentration [g·L^{-1}]
$EBCT$	Empty bed contact time [min]
k_{AB}	Adams–Bohart kinetic constant [L·mg^{-1} min^{-1}]
k_{Th}	Thomas rate constant [mg·L^{-1}]
k_{YN}	Yoon–Nelson rate constant [min^{-1}]
K_a	Rate constant [L·mg^{-1} min^{-1}]
m_{total}	Total amount of urea fed to the column [mg]
N	Number of sorption runs
N_0	Saturation concentration [mg·L^{-1}]
q_c	Column capacity [mg]
q_{eq}	Equilibrium uptake or maximum column capacity [mg·g^{-1}]
q_{exp}	Experimental uptake or maximum column capacity [mg·g^{-1}]
q_{pred}	Predicted uptake or maximum column capacity [mg·g^{-1}]
q_0	Maximum solid-phase concentration of the solute [mg·g^{-1}]
Q	Flow rate [mL·min^{-1}]
R^2	Coefficient of determination
t_b	Breakthrough time [min]
t_e	Bed exhaustion time [min]
t_{total}	Total flow time [min]
U_0	Linear velocity from Adams–Bohart model [cm·min^{-1}]
v	Flow rate [mL·min^{-1}]
V	Velocity [cm min^{-1}]
Δt	Mass transfer zone [min]
t or τ_{exp}	Time required for 50% of adsorbate break-through [min]
X	Total mass of adsorbent in the column [g]
Y	Linear velocity [cm min^{-1}]
Z	Bed height [cm]
Z_m	Length of the mass transfer zone [cm]

caused adverse effects on human health [14], and also represent a continued economic loss to the farmer as unavailable soil nutrients.

Indeed, several studies have been performed on developing pathways to minimize these losses; they have focused on dietary manipulation [15–18], use of inhibitors [19,20] and in-situ soil amendment with charcoal/biochar following the application of urine [21,22]. The objective of these studies has either been restricted to reducing ammonia volatilization or increasing the availability of ammonia-N subsequent to urine application in soils. However, the direct application of cattle urine, a fast acting fertilizer, has its downsides of increased soil salinity, acidity and conductivity and in some cases, crop losses

[23,24]. Enclosure experiments in various studies have indicated that 4–41% of the N applied from cattle urine may volatilize following its application on arable soils [25,26]. Hence, this study argues that an alternative strategy to inhibit such emissions while simultaneously recovering urea-N from cattle urine (ex-situ) for subsequent use as fertilizer could be through the use of physical adsorption processes.

Biosorption using activated carbon (AC) prepared from renewable agro-waste can be seen as a promising method for urea recovery [27–30]. In our earlier investigations, batch experiments were performed to demonstrate the efficiency of AC toward urea recovery from urine [31–33]. The principal objective of the present study was to demonstrate a continuous process to recover urea from cattle urine through adsorption using AC prepared from coconut shells. To perform this, we focus on cyclic sorption/desorption that employs packed-bed column which makes effective utilization of concentration difference, adsorbent capacity and, hence, results in better quality effluent streams [34]. Moreover, a continuous packed-bed column also has process engineering advantages of ease in scale-up of the investigated procedure and can treat high volumes of influent streams using a definite quantity of adsorbent. On the contrary, earlier studies have shown that regeneration of AC and the cost of the sorbent is relatively high, which subsequently limits its application. To this effect, immobilization of AC onto a supporting material offers an efficient solution to the problems involved in separation processes [35]. Given their low cost, mechanical strength, and ease of surface modification, this study uses etched glass beads as the support material [36]; indeed, glass beads have found application as a support material for several other immobilization studies [36–39]. In particular, immobilization is well suited for non-destructive recovery of substances and is relatively resistant in chemical environment [35,40–42]. Hence, this study employs immobilization of the prepared AC onto etched glass beads to ease post-experimental recovery of the adsorbed urea.

2. Materials and methods

2.1. Urine: collection and characterization

The urine specimen was collected from four Indian dairy cows (diet consisted exclusively of grazed grass) while the animal was indoor for milking. Collection was carried out two to three times per day for a period of 7 consecutive days using polyethylene buckets. The urine was immediately transferred to the laboratory in sterile polypropylene containers and stored at −15°C until required. Following the period of collection, all samples were thawed, thoroughly mixed and immediately utilized in the adsorption column. Initially, the urine was characterized for its total-N and urea-N concentrations.

2.2. Sorbent preparation

2.2.1. Activated carbon

Activated carbon (AC) was prepared from coconut shells as described in an earlier study [31]. Initially, coconut shells were washed with distilled water, air dried at 110°C for 24 h in a tray dryer and crushed in a roll mill to particle size fractions of
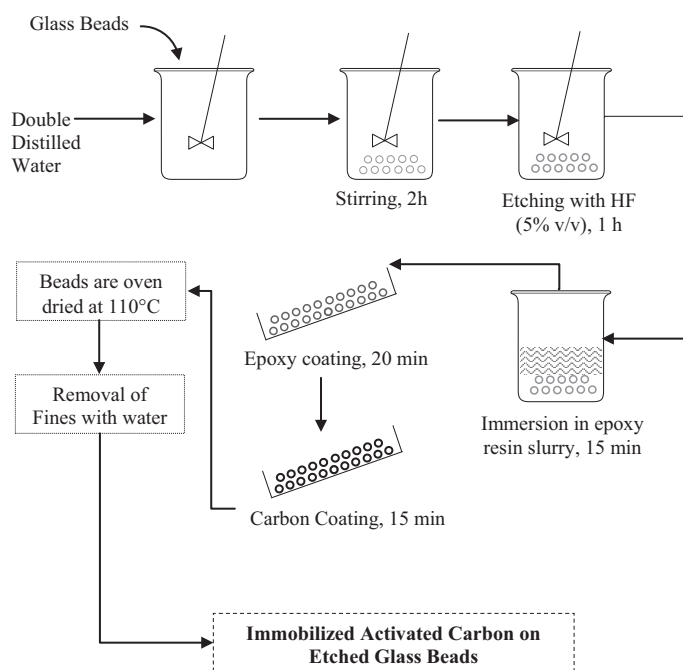
Fig. 1. Schematic diagram for immobilization procedure of the AC.

1–2 cm. Subsequently, they were subjected to microwave activation in a domestic microwave (CE104VD – Samsung, Malaysia) at an output power of 360 W for 15 min and further carbonized in an industrial high temperature furnace (T-14/HTF-1400, Technico, India) at 500 °C (heating rate of 22 °C min^{-1}) for 2 h. The AC obtained was further reduced to a size of 100 mesh (1 mm) using a ball mill operated at 83 rev·min^{-1} (Deepthi Enterprise, Bangalore, India) and stored in plastic air-tight containers for further analyses.

2.2.2. Immobilization

Initially, the procured glass beads (ϕ 1.5 and 2.2 cm) were washed with double distilled water for 2 h. Subsequently, the glass beads were etched with dilute hydrofluoric acid (5% v/v) for 1 h. Slurry of synthetic epoxy resin in deionized water (10% v/v) was prepared and continuously mixed for 30 min. The etched glass beads were then immersed in the slurry for 15 min. Following this, uniform epoxy coating was ensured by using a Gel Rocker (Xitij Instruments Pvt. Ltd, Pune, India) for 20 min; lastly, the AC prepared was surface coated and immobilized in the Gel Rocker for 15 min and left for a while to ensure no air bubbles are present. The AC coated glass beads were oven dried at 110 °C for 2 h and washed with doubled distilled water for the removal of any free AC particles prior to their use in the column. Thickness of the AC film on the glass beads was 2 mm. The immobilization procedure followed is illustrated in Fig. 1.

2.3. Adsorption experiments

A Pyrex glass column of 80 cm height and internal diameter of 4 cm served as the sorption unit (Fig. 2). The ends of the column were provided with a sintered glass filter, stainless steel sieve plate and glass wool. Glass beads immobilized with AC were then randomly packed into the column. The column was connected to two covered liquid-holding tanks to hold the working solutions, cattle urine and deionized water. Prior to the sorption experiment, the bed was rinsed with deionized water in
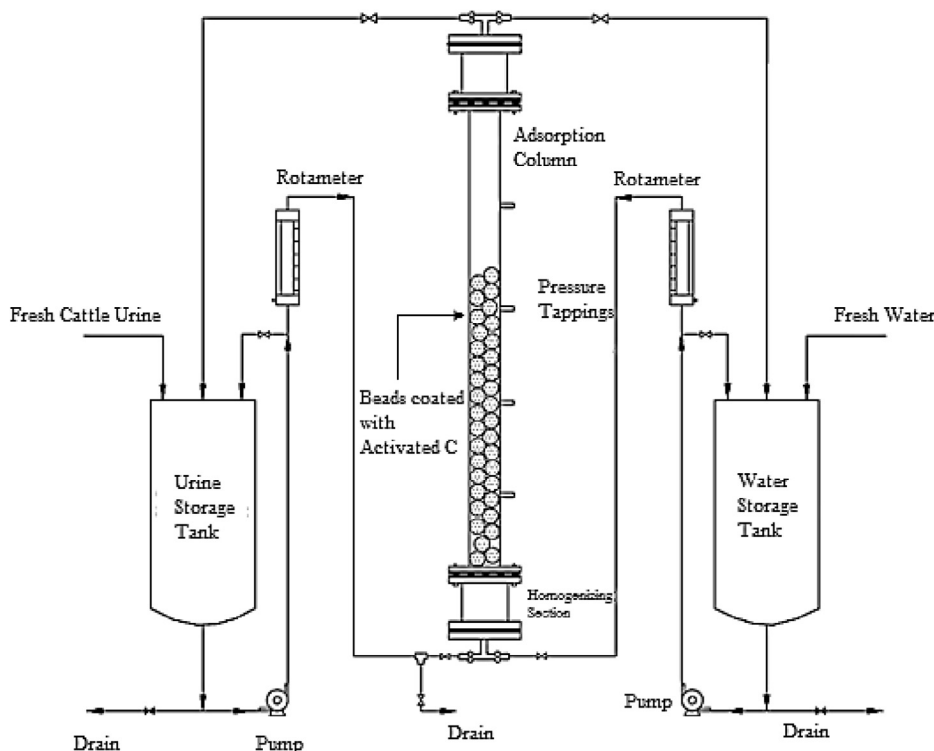

Fig. 2. Schematic diagram for urea sorption onto immobilized AC in continuous packed column.

up-flow mode until no air bubbles could be seen [43]. Following this, sorption experiments were performed by pumping cattle urine in downward flow mode using peristaltic pump (PP10EX, Miclins, India). To estimate the effluent urea concentration, at every 5 min time interval, 3 mL aliquots were withdrawn, filtered through a 0.45 μm Ministat filter (Sartorius Stedim Biotech GmbH, Germany) and monitored for change in absorbance (at 430 nm) by a UV-Vis spectrophotometer [44]. This process was repeated until the establishment of sorption equilibrium. An array of experiments was performed on the column to understand the sorption dynamics by varying initial urea concentration in urine (20%–2.3 g·L⁻¹, 40%–4.6 g·L⁻¹, 60%–6.9 g·L⁻¹, 80%–9.2 g·L⁻¹ and 100%–11.5 g·L⁻¹), inlet adsorbate flow rate (2–10 L·h⁻¹) and diameter of the glass beads (1.5 and 2.2 cm). Initial urea concentration was varied through dilution of cattle urine with distilled water. The column was operated under laboratory conditions at 23 ± 1°C; the temperature was fixed based on the results of previous investigations where urea uptake was found to decrease with increasing temperature [32].

2.4. Regeneration

Column regeneration is crucial to process economics. It must allow for production of small volumes of sorbate concentrates to ease post-column urea recovery without damaging the sorbent capacity making it reusable for several adsorption–desorption cycles [45]. In order to recover the adsorbed urea, regeneration studies were performed on the exhausted column. Given the unsuitability of high temperature thermal regeneration process or chemical reagents toward recovery of volatile organics [46], the present study examines the use of deionized water as a suitable desorption fluid. In our previous batch experiments on carbon regeneration, deionized was shown to be a promising solvent for urea desorption [33]. Hence, deionized water was pumped in up-flow mode at 2 L·h⁻¹ (based on initial studies) through the saturated column with eluted urea concentration measured similar to the procedure followed for the adsorption runs. Regeneration was ceased when a 5% loss in sorption capacity of the regenerated AC was observed. In all the experimental runs, this cut-off value (5%) was attained by the end of the seventh adsorption–desorption cycle.

2.5. Dynamic column analysis

In a column adsorption system, maximum adsorption and concentration of adsorbate molecules occur in the adsorbent positioned closest to the inlet sorbate flow. As the sorbate solution passes through the packed column, this adsorption zone moves further down [47]. After its breakthrough at the exhaustion point, this zone moves out of the column where exit concentration becomes equal to that of the inlet feed. The time for breakthrough and shape of the breakthrough curves are very important to understand the dynamics and performance of the column. The breakthrough curves were plotted to express the relation between the ratio of effluent (C_t; mg·L⁻¹) and feed urea concentration (C_0; mg·L⁻¹) with time (t; min). The adsorbed urea concentration (C_{ads}; mg·L⁻¹) was calculated as $C_{ads} = C_0 - C_t$. Further, area under the breakthrough curve (A) obtained by

integrating the adsorbed urea concentration with time was used to find the maximum column capacity (q_c; g). The total adsorbed urea in the column for a given flow rate (Q; mL·min⁻¹), inlet feed concentration and column operating time (t_{total}; min) was determined by Eq. 1 [48].

$$q_c = \left(\frac{QA}{1000}\right) = \frac{Q}{1000} \int_0^{t_{total}} C_{ads} dt \tag{1}$$

The total urea sent (m_{total}; g) to the column was calculated as in Eq. 2 [49]. Further, the equilibrium urea uptake (q_e; mg·g⁻¹), defined as the total amount of urea adsorbed by the column (q_c; mg·g⁻¹) per gram of sorbent (X) at the end of total flow time, was estimated by Eq. 3 [40]. The total urea adsorption (%) was calculated from Eq. 4 [35].

$$m_{total} = C_0 \cdot Q \cdot \left(\frac{t_{total}}{1000}\right) \tag{2}$$

$$q_e = \left(\frac{q_c}{X}\right) \tag{3}$$

$$\% \ adsorption = \left(\frac{q_c}{m_{total}}\right) \cdot 100 \tag{4}$$

The mass transfer zone (Δt; min) is the difference between the bed exhaustion time t_e (time for effluent urea concentration to reach 95% of the influent concentration) and the breakthrough time t_b [50]. The length of the mass transfer zone (Z_m) was calculated by Eq. 5, where Z is the bed height [51]. The empty bed residence time ($EBRT$; min) is the time required for the sorbate solution to fill the empty column (Eq. 6).

$$Z_m = Z \cdot \left(1 - \frac{t_b}{t_e}\right) \tag{5}$$

$$EBRT = \frac{Bed \ volume}{Volumetric \ flow \ rate \ of \ the \ liquid} \tag{6}$$

2.6. Sorption modeling

To describe the sorption of various sorbate molecules, several empirical models have been developed [40,47,52]. In the present investigation, the dynamic behavior of the column was predicted with Adams–Bohart, Thomas and Yoon–Nelson models. The Adams–Bohart model describes the initial section of the breakthrough curves between 10% and 50% of the saturation points and assumes that adsorption rate is proportional to both the residual capacity of the adsorbent and the concentration of the adsorbing species [53] and is expressed as in Eq. 7.

$$ln\left(\frac{C_t}{C_0}\right) = k_{AB}C_0 t - \left(\frac{k_{AB}N_0 Z}{U_0}\right) \tag{7}$$

where C_0 and C_t (mg·L⁻¹) are inlet and effluent urea concentration, U_o is the linear velocity (cm·min⁻¹) defined as the ratio of volumetric flow rate to bed cross-sectional area, k_{AB} is the kinetic constant (L·mg⁻¹ min⁻¹), and N_0 is the saturation concentration (mg·L⁻¹). The Thomas model suited for systems

where breakthrough occurs immediately following column operation was used in its linearized form through Eq. 8 [54]. The kinetic coefficient k_{Th} (L·mg^{-1}h^{-1}) and maximum solid-phase concentration of urea in the column, q_o (mg·g^{-1}), were determined by the plot of C_t/C_0 versus time.

$$ln\left(\frac{C_0}{C_t}-1\right)=\left(\frac{k_{Th}q_0m}{Q}\right)-k_{Th}C_0t \qquad (8)$$

The Yoon–Nelson model, widely used for single-component systems, is based on the assumption that rate of decrease in probability of sorption of adsorbate molecule is proportional to the probability of the adsorbate adsorption and adsorbate breakthrough on the adsorbent [55]. The linearized form of the model was used as expressed in Eq. 9. A linear plot of ln(C_t/(C_0 - C_t)) against time (t) was used to determine k_{YN}, the Yoon–Nelson rate constant (min^{-1}) and τ, the time required (min) for 50% of adsorbate breakthrough.

$$ln\left(\frac{C_t}{C_0-C_t}\right)=k_{YN}t-\tau k_{YN} \qquad (9)$$

2.7. Data analysis and processing

All the experiments were performed in triplicate. Urea absorbance measurements were performed by UV-vis spectrophotometry for all experimental runs at a photometric accuracy of ±0.002 Abs, photometric repeatability of ±0.001 Abs and noise level of 0.002 Abs. The limit of detection (LoD) and limit of quantitation (LoQ) were calculated based on standard deviation of the responses and the slope of three independent analytical curves to be 0.1002 and 0.303 mg·L^{-1}, respectively. Statistical analysis of the sorption runs was performed using MATLAB® and the deviations were within 5%. For all visualizations, mean values have been used and reported. Further, in order to determine which sorption model best described the urea sorption within the column, the coefficient of determination (R^2), root mean square error ($RMSE$) and chi-square (χ^2) were calculated (Eq. 10 and Eq. 11). $q_{exp,i}$ and $q_{pre,i}$ are the 'ith' experimental and predicted urea sorption capacity (mg·g^{-1}), respectively; n is the number of observations and N is the number of constants in the sorption model. Further, to better gauge the goodness of fit of the experimental data against the sorption models, normalized deviation and normalized standard deviation were also calculated as in Eq. 12 and Eq. 13 [56].

$$RMSE=\sqrt{\left[\frac{1}{n}\sum_{i=1}^{n}\left(q_{exp,i}-q_{pred,i}\right)^2\right]} \qquad (10)$$

$$\chi^2=\frac{\sum_{i=1}^{N}\left(q_{exp,i}-q_{pred,i}\right)^2}{n-N} \qquad (11)$$

$$Normalized\ Deviation=\frac{100}{n}\sum\left|\frac{q_{e(exp)}-q_{e(pred)}}{q_{e(exp)}}\right| \qquad (12)$$

Table 1
Physical and chemical properties of the prepared AC.

Property	Value
Apparent density (g·cm^{-3})	0.39
Yield (%)	25.81
pH	8.23
Electrical conductivity (dS·m^{-1})	0.12
Ash content (%)	0.63
Carbon (%)	49.51
Sulfur (%)	0.58
Hydrogen (%)	7.11
Nitrogen + oxygen (%)*	42.17
Surface area (BET; m^2·g^{-1})	1032
Pore volume (cm^3·g^{-1})	0.28
Size of AC support (ϕ, cm)	1.5, 2.2
Thickness of immobilized AC film (mm)	2

* Estimated by difference

$$Normalized\ Std\ Deviation=100\sqrt{\frac{\sum\left(q_{e(exp)}-q_{e(pred)}\right)\big/q_{e(exp)}\right)^2}{n}} \qquad (13)$$

3. Results and discussion

3.1. Sorbate and sorbent characterization

The total N concentration of the urine samples determined by Kjeldahl analysis was found to be 6.9 g·L^{-1} while urea-N was 5.38 g·L^{-1}. Initial urea concentration of the cattle urine was hence found to be 11.5 g·L^{-1} and urea-N contributed to 77.9% of the total N, a proportion consistent with observations made in other studies [57,58]. It was observed that *ca* 16% of the N gets lost as ammonia-N if urine is stored at room temperature; however, no loss of ammonia-N was noticed during storage at −15°C. Moreover, The physical and chemical properties of the prepared AC were determined as described earlier [31] and have been summarized in Table 1.

3.2. Influence of flow rate

Influence of flow rate (2–10 L·h^{-1}) on the column breakthrough was examined at an initial urea concentration of 60% for a column packed with 1.5 cm AC spheres (Fig. 3). All flow rates considered in the study gave gentle breakthrough curves for the prepared AC. As seen in the figure, breakthrough occurs faster as flow rate increases, with breakthrough time decreasing from 112 to 65 min. Moreover, the corresponding percentage adsorption (or urea removal efficiency) was seen to drop from 83.53 to 79.81%. This is expected, as lower flow rate (or high *EBRT*) allows slower diffusion of the sorbate ensuring that the sorbent has greater time to come in contact with the urea molecules [40]. However, even at high flow rates, the contact time was sufficient enough to allow efficient urea recovery from the column (Table 2). In addition, the resultant column and equilibrium adsorption capacity were found to increase as flow rate increased from 2 L·h^{-1} (298.1 mg·g^{-1}) to 10 L·h^{-1} (918.6 mg·g^{-1}). This suggested that the process was external mass transfer controlled with higher flow rate decreasing the film resistance [59]. Since the percentage urea removal did not differ
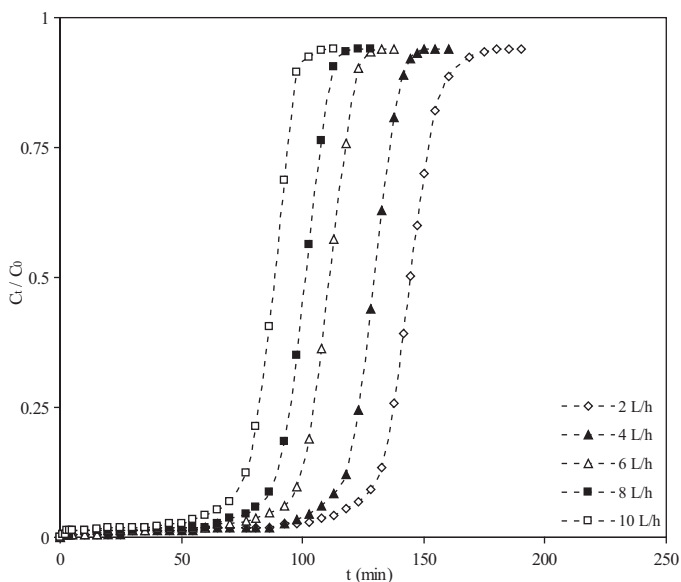
Fig. 3. Column breakthrough curves at various flow rates (C_0: 60%, glass sphere diameter: 1.5 cm).

Fig. 4. Column breakthrough curves at various inlet concentrations (glass sphere size = ϕ 2.2 cm, flow rate = 6 L·h^{-1}).

significantly for the flow rates investigated, through observations of the column breakthrough times and equilibrium sorption capacity, 8 L·h^{-1} is suggested as a good sorbate flow rate.

3.3. Influence of concentration

The effect of varying initial urea concentration in the sorbate (20–100%) examined at a flow rate of 10 L·h^{-1} with AC immobilized on glass spheres of 2.2 cm diameter is shown through the breakthrough curve. As seen in Fig. 4, breakthrough time decreased (123 to 46 min) with increasing urea concentration and sharp breakthrough curves were observed at high concentration, indicating the diffusion was concentration dependent [40]. At higher inlet concentration, the urea loading rate increases which subsequently increases the driving force for mass transfer and decreases the adsorption zone length [45].
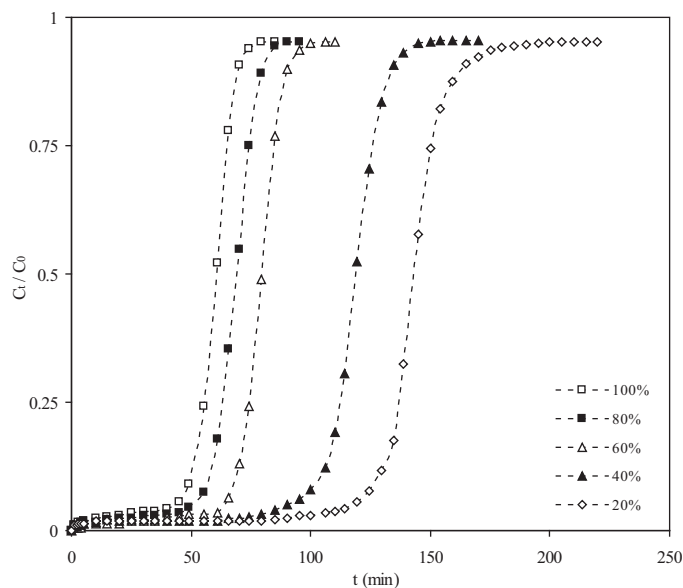
Moreover, the adsorption capacity is expected to increase due to higher concentration difference, driving the mass transfer, and a similar trend was observed with highest sorption (878.7 mg·g^{-1}) occurring at 100% feed concentration. In addition, as shown in Table 2, the removal efficiency was higher for lower inlet urea concentration, with inlet concentration of 20 and 100% resulting in 79.58 and 73.42% removal, respectively. The results were in agreement with other studies on packed-bed adsorption systems for AC [40,45,60]. Based on these observations, 60% initial concentration is suggested as the operating condition for urea removal from cattle urine.

3.4. Influence of carbon support

The effect of size of AC support on the column breakthrough was examined by varying the diameter of the etched glass beads

Table 2
Effect of various process variables on operation of the immobilized sorption column.

Run	Initial conc. (%)	Flow rate (L·h^{-1})	Support size (cm)	t_b (min)	t_e (min)	Δt (min)	EBCT (min)	q_c (g)	q_e† (mg·g^{-1})	Adsorption (%)
1	20	6	2.2	123	210	87	9.05	28	357.4 ± 4.23	79.58
2	40			98	160	62	9.05	46	580.3 ± 5.65	78.84
3	60			66	100	34	9.05	49	596.2 ± 4.95	77.47
4	80			51	85	34	9.05	52	658.3 ± 6.46	74.45
5	100			46	80	34	9.05	56	713.2 ± 6.26	73.42
6	20	10	1.5	116	190	74	5.43	42	538.6 ± 5.50	74.09
7			2.2	107	185	78	5.43	44	480.6 ± 4.16	73.82
8	60		1.5	65	100	35	5.43	80	918.6 ± 8.25	79.81
9			2.2	75	95	20	5.43	72	868.1 ± 7.82	78.06
10	100		1.5	41	80	39	5.43	92	991.5 ± 8.42	77.15
11			2.2	33	70	37	5.43	69	878.7 ± 6.18	62.16
12	60	2	1.5	112	180	68	27.1	28	298.1 ± 4.35	83.53
13		4		104	155	51	13.5	48	517.2 ± 5.85	82.13
14		6		85	130	45	9.05	61	660.9 ± 5.65	81.68
15		8		78	120	42	6.78	74	802.8 ± 7.78	80.55

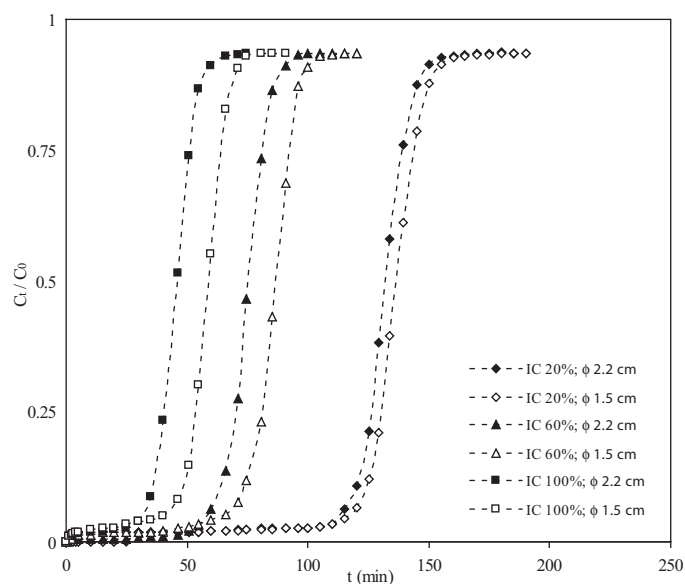† Values of mean ± standard error, *n-3* per treatment group.

Fig. 5. Column breakthrough curves at various glass sphere sizes and inlet concentration (flow rate = 10 L·h^{-1}).

(1.5 and 2.2 cm) at a flow rate of 10 L·h^{-1} and three different initial urea concentrations (20, 60 and 100%). As seen through the breakthrough curves (Fig. 5), a larger adsorbent support size leads to an earlier breakthrough with the slope of the curves increasing with a decrease in the diameter of the glass beads. The smaller the diameter of the support, the higher is the total external surface area per unit volume available for initial mass transfer and, subsequently, urea sorption [59]. The larger the support, the smaller is the surface area available and, hence, initial mass transfer rate with an earlier breakthrough. As seen in Table 2, for smaller support (φ 1.5 cm), the capacity was higher due to faster rate of adsorption. As expected, the same trend was also followed for varied inlet urea concentration.

3.5. Modeling the column breakthrough

The sorption data were tested against various kinetic models to determine model parameters for urea adsorption on AC

immobilized onto glass beads and is presented in Table 3. As seen, both k_{Th} and q_0 were found to increase with flow rate although lesser urea removal occurs. Moreover, deviations of the experimental data against the predicted values were observed at higher flow rates. The increase in inlet concentration and size of the AC support allowed for higher urea adsorption. For the Thomas model, the correlation between C_t/C_0 and time was found to be significant (Eq. 8) with R^2 values ranging from 0.82 to 0.95. This is expected as the Thomas model suits sorption where diffusion (both, external and internal) is not the limiting step [35]. For the Yoon–Nelson model, the rate velocity constant (k_{YN}) increased while time for 50% breakthrough (τ) decreased for both, increasing flow rate and urea concentration. Similar observations have been reported by Ahmad and Hameed [40] as well as Aksu and Gönen [35]. Moreover, the Yoon–Nelson model was able to provide good correlation to the effect of AC support size, with τ values significantly similar to experimental observations. The Adams–Bohart model as applied through Eq. 7 was used to determine k_{AB} and N_0 values along with the coefficient of determination ($R^2 > 0.86$) as shown in Table 3. N_0 increased with sorbate flow rate and initial urea concentration although no significant effect was seen with change in AC support size except at 100% initial urea concentration in the sorbate. Moreover, k_{AB} was influenced by flow rate further indicating that sorption kinetics was dominated by external mass transfer in the initial stages. At various conditions examined, both the Thomas and Adams–Bohart model provided good fit ($R^2 > 0.82$) to the column experimental data. For the Thomas, Yoon–Nelson and Adams–Bohart models, the normalized deviation was calculated as 5.52, 14.58 and 5.14 (Eq. 12) and the normalized standard deviation was calculated as 7.04, 48.35 and 6.82 (Eq. 13), respectively. Hence it can be concluded that the urea sorption process for the packed-bed column was better described by the Adams–Bohart model.

3.6. Regeneration studies

Column regeneration studies were performed for seven cycles of adsorption–desorption using deionized water pumped

Table 3
Model parameters and goodness of fit of the experimental sorption data against various kinetic equations.

Run[†]	Thomas model					Yoon–Nelson model					Adams–Bohart model				
	k_{Th}	q_0	R^2	RMSE	χ^2	k_{YN}	τ	R^2	RMSE	χ^2	k_{AB}	N_0	R^2	RMSE	χ^2
1	0.019	361.9	0.842	1.093	1.274	0.037	149.3	0.842	1.093	1.274	0.012	43.52	0.866	0.632	0.426
2	0.012	584.2	0.824	1.149	1.434	0.046	120.5	0.824	1.150	1.434	0.007	51.03	0.868	0.617	0.825
3	0.013	578.8	0.853	1.084	1.328	0.074	79.62	0.853	1.063	1.273	0.008	67.91	0.912	0.532	0.318
4	0.011	619.5	0.893	0.896	0.925	0.084	67.45	0.893	0.896	0.925	0.007	75.19	0.906	0.562	0.362
5	0.009	703.1	0.868	0.952	1.057	0.088	58.01	0.868	0.951	1.057	0.005	86.07	0.919	0.453	0.237
6	0.021	482.6	0.858	1.267	1.727	0.040	140.8	0.883	1.267	1.727	0.013	68.62	0.877	0.629	0.845
7	0.023	539.6	0.876	1.148	1.423	0.044	133.6	0.876	1.148	1.423	0.015	63.55	0.897	0.613	0.807
8	0.011	885.3	0.851	1.095	1.332	0.064	86.11	0.816	1.085	1.332	0.007	120.8	0.901	0.506	0.287
9	0.014	959.1	0.879	1.165	1.521	0.082	79.15	0.879	1.165	1.522	0.009	113.0	0.902	0.762	0.647
10	0.009	991.9	0.862	0.826	0.803	0.086	57.88	0.882	0.806	0.758	0.006	138.1	0.936	0.385	0.173
11	0.012	914.3	0.877	0.825	0.808	0.114	45.27	0.921	0.804	0.718	0.007	113.3	0.897	0.592	0.412
12	0.007	303.5	0.888	0.929	0.927	0.042	147.6	0.888	0.929	0.927	0.005	40.13	0.934	0.480	0.247
13	0.008	436.4	0.947	1.138	1.409	0.048	130.1	0.828	1.138	1.409	0.006	70.85	0.897	0.588	0.376
14	0.009	692.1	0.821	1.082	1.298	0.054	112.1	0.820	1.082	1.298	0.006	90.55	0.906	0.526	0.305
15	0.010	834.8	0.838	1.087	1.322	0.057	101.5	0.818	1.087	1.325	0.007	110.7	0.894	0.552	0.339

[†] Specific experimental conditions for each run have been provided in Table 2; R^2: coefficient of determination; RMSE: root mean square error; χ^2: chi-square.
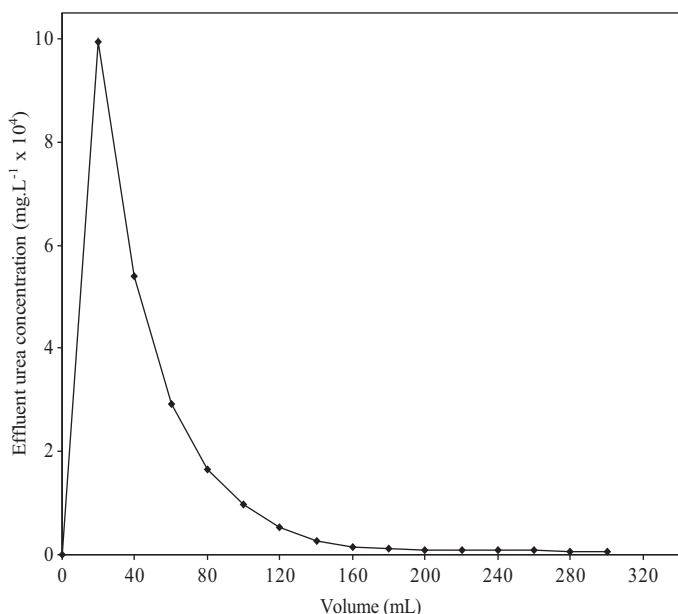
Fig. 6. Desorption curve depicting the collected volume of eluent against the concentration of recovered urea.

up-flow at 2 L·h^{-1}. Fig. 6 shows the trend for collected volume of eluent against the concentration of recovered urea from the column. The results indicate a sharp increase in urea concentration at the commencement of deionized water elution, with maximum concentration of 9.94 g·mL^{-1} which was 11-fold the inlet urea concentration. During the elution, 50% urea desorption was achieved using 55 mL eluent volume with urea recovery attaining equilibrium at ~120 mL deionized water. It was observed that nearly 95% of the adsorbed urea can be easily eluted and recovered from the column indicating the reversible nature of the urea sorption as well as the ability of the sorbent to be used multiple times. A loss of 5% in uptake capacity of the sorbent was observed at the end of seven cycles.

In order to recover or utilize the concentrated urea from the eluant, two pathways are suggested: direct application (following dilution with water) as a liquid fertilizer on arable land or through drying and crystallization operations to produce solid urea as this would ease its storage and transportation. It is acknowledged here that the purpose of the regeneration experiments was to demonstrate the reuse potential of the column as well as show a pathway for urea recovery. Given the non-selective nature of any physical adsorption process, further purification would be required in order to meet regulatory standards or market specifications.

4. Conclusions

Coconut shell based AC immobilized onto etched glass beads was effective in recovering urea from cattle urine. The favorable operating parameters were sorbate flow: 8 L·h^{-1}, initial urea concentration: 60%, and glass bead support size: 1.5 cm. The column allowed an equilibrium adsorption of 802.8 mg·g^{-1}, column capacity of 74.2 g and >80% urea recovery. De-ionized water recovered nearly 95% of the adsorbed

urea during regeneration. Over seven sorption–desorption cycles, loss in uptake capacity of sorbent was less than 5%. Further, it is also the recommendation of this study that the results obtained by various authors working on nutrient recovery technologies in the purview of sustainable agriculture be analyzed in a systems perspective and with the aid of tools like life cycle analysis. A systemic analysis of the socio-economic and environmental benefits as well as costs of the proposed technological solutions against the conventional (industrial) fertilizer manufacturing process would allow two significant conclusions to be drawn: (i) it would reveal where, and to what extent, different steps in the nutrient cycle could be improved by the proposed solution(s); (ii) further, it could potentially establish the overall competitiveness of the solutions against conventional processes and provide evidence to support the notion of alternative fertilization.

References

[1] E.B. Barbier, Economics, natural-resource scarcity and development: conventional and alternative views, Routledge, London, 2013, pp. 1–22. ISBN 13:978-0-203-76890-7.

[2] P. Potter, N. Ramankutty, E.M. Bennett, S.D. Donner, Characterizing the spatial patterns of global fertilizer application and manure production, Earth Interactions 14 (2) (2010) 1–22, doi:10.1016/S1352-2310(97)00043-5.

[3] J.A. Foley, R. DeFries, G.P. Asner, C. Barford, G. Bonan, S.R. Carpenter, et al., Global consequences of land use, Science 309 (5734) (2005) 570–574, doi:10.1126/science.1111772.

[4] J.N. Galloway, The global nitrogen cycle: changes and consequences, Environ. Pollut. 102 (1) (1998) 15–24, doi:10.1016/S0269-7491(98)80010-9.

[5] D. Tilman, K.G. Cassman, P.A. Matson, R. Naylor, S. Polasky, Agricultural sustainability and intensive production practices, Nature 418 (6898) (2002) 671–677, doi:10.1038/nature01014.

[6] M. Ganesapillai, P. Simha, S.S. Beknalkar, D.M.R. Sekhar, Low-grade rock phosphate enriched human urine as novel fertilizer for sustaining and improving agricultural productivity of Cicer arietinum, Sustain. Prod. Consum. 6 (2016) 62–66, doi:10.1016/j.spc.2016.01.005.

[7] N. Gilbert, Environment: the disappearing nutrient, Nat. News 461 (7265) (2009) 716–718, doi:10.1038/461716a.

[8] G. Haq, H. Cambridge, Exploiting the co-benefits of ecological sanitation, Curr. Opin. Environ. Sustain. 4 (4) (2012) 431–435, doi:10.1016/j.cosust.2012.09.002.

[9] G. Langergraber, E. Muellegger, Ecological sanitation – a way to solve global sanitation problems?, Environ. Int. 31 (3) (2005) 433–444, doi:10.1016/j.envint.2004.08.006.

[10] V.H. Varel, J.A. Nienaber, H.C. Freetly, Conservation of nitrogen in cattle feedlot waste with urease inhibitors, J. Anim. Sci. 77 (5) (1999) 1162–1168, doi:/1999.7751162x.

[11] S.C. Jarvis, Nitrogen cycling and losses from dairy farms, Soil Use Manage. 9 (3) (1993) 99–104, doi:10.1111/j.1475-2743.1993.tb00937.x.

[12] S.O. Petersen, S.G. Sommer, O. Aaes, K. Søegaard, Ammonia losses from urine and dung of grazing cattle: effect of N intake, Atmos. Environ. 32 (3) (1998) 295–300, doi:10.1016/S1352-2310(97)00043-5.

[13] A. Fangmeier, A. Hadwiger-Fangmeier, L. Van der Eerden, H.J. Jäger, Effects of atmospheric ammonia on vegetation-a review, Environ. Pollut. 86 (1) (1994) 43–82, doi:10.1016/0269-7491 (94)90008-6.

[14] C.I. Davidson, R.F. Phalen, P.A. Solomon, Airborne particulate matter and human health: a review, Aerosol Sci. Technol. 39 (8) (2005) 737–749, doi:10.1080/02786820500191348.

[15] N.A. Cole, R.N. Clark, R.W. Todd, C.R. Richardson, A. Gueye, L.W. Greene, et al., Influence of dietary crude protein concentration and source on potential ammonia emissions from beef cattle manure, J. Anim. Sci. 83 (3) (2005) 722–731, doi:/2005.833722x.

[16] J. Dijkstra, O. Oenema, J.W. van Groenigen, J.W. Spek, A.M. van Vuuren, A. Bannink, Diet effects on urine composition of cattle and N_2O emissions, Animal 7 (2) (2013) 292–302, doi:10.1017/ S1751731113000578.

[17] T.H. Misselbrook, J.M. Powell, G.A. Broderick, J.H. Grabber, Dietary manipulation in dairy cattle: laboratory experiments to assess the influence on ammonia emissions, J. Dairy Sci. 88 (5) (2005) 1765–1777, doi:10.3168/jds.S0022-0302(05)72851-4.

[18] B. Van Der Stelt, P.C.J. Van Vliet, J.W. Reijs, E.J.M. Temminghoff, W.H. Van Riemsdijk, Effects of dietary protein and energy levels on cow manure excretion and ammonia volatilization, J. Dairy Sci. 91 (12) (2008) 4811–4821, doi:10.3168/jds.2006-449.

[19] J. Singh, A. Kunhikrishnan, N.S. Bolan, S. Saggar, Impact of urease inhibitor on ammonia and nitrous oxide emissions from temperate pasture soil cores receiving urea fertilizer and cattle urine, Sci. Total Environ. 465 (2013) 56–63, doi:10.1016/j.scitotenv.2013.02.018.

[20] M. Zaman, S. Saggar, J.D. Blennerhassett, J. Singh, Effect of urease and nitrification inhibitors on N transformation, gaseous emissions of ammonia and nitrous oxide, pasture yield and N uptake in grazed pasture system, Soil Biol. Biochem. 41 (6) (2009) 1270–1280, doi:10.1016/ j.soilbio.2009.03.011.

[21] A. Taghizadeh-Toosi, T.J. Clough, R.R. Sherlock, L.M. Condron, A wood based low-temperature biochar captures NH_3-N generated from ruminant urine-N, retaining its bioavailability, Plant Soil 353 (1–2) (2012) 73–84, doi:10.1007/s11104-011-1010-9.

[22] Y. Yao, B. Gao, M. Zhang, M. Inyang, A.R. Zimmerman, Effect of biochar amendment on sorption and leaching of nitrate, ammonium, and phosphate in a sandy soil, Chemosphere 89 (11) (2012) 1467–1471.

[23] A.F. Bouwman, K.W. Van Der Hoek, Scenarios of animal waste production and fertilizer use and associated ammonia emission for the developing countries, Atmos. Environ. 31 (24) (1997) 4095–4102, doi:10.1016/S1352-2310(97)00288-4.

[24] K.H. Orwin, J.E. Bertram, T.J. Clough, L.M. Condron, R.R. Sherlock, M. O'Callaghan, et al., Impact of bovine urine deposition on soil microbial activity, biomass, and community structure, Appl. Soil Ecol. 44 (1) (2010) 89–100, doi:10.1016/j.apsoil.2009.10.004.

[25] D.W. Bussink, O. Oenema, Ammonia volatilization from dairy farming systems in temperate areas: a review, Nutr. Cycl. Agroecosys. 51 (1) (1998) 19–33, doi:10.1023/A:1009747109538.

[26] D.C. Whitehead, N. Raistrick, The volatilization of ammonia from cattle urine applied to soils as influenced by soil properties, Plant Soil 148 (1) (1993) 43–51, doi:10.1007/BF02185383.

[27] A. Bhatnagar, A.K. Jain, A comparative adsorption study with different industrial wastes as adsorbents for the removal of cationic dyes from water, J. Colloid Interface Sci. 281 (1) (2005) 49–55, doi:10.1016/j.jcis.2004.08.076.

[28] J.M. Dias, M.C.M. Alvim-Ferraz, M.F. Almeida, J. Rivera-Utrilla, M. Sánchez-Polo, Waste materials for activated carbon preparation and its use in aqueous-phase treatment: a review, J. Environ. Manage. 85 (4) (2007) 833–846, doi:10.1016/j.jenvman.2007.07.031.

[29] R. Malik, D.S. Ramteke, S.R. Wate, Adsorption of malachite green on groundnut shell waste based powdered activated carbon, Waste Management 27 (9) (2007) 1129–1138, doi:10.1016/j.wasman.2006 .06.009.

[30] S. Prithvi, Use of urea adsorbed KOH-activated Napier grass biochar for soil conditioning – A step towards biochar tailoring, Spanish J. Rural Dev. 5 (4) (2014) doi:10.5261/2014.GEN4.04.

[31] M. Ganesapillai, P. Simha, A. Gugalia, Recovering urea from human urine by bio-sorption onto microwave activated carbonized coconut shells: equilibrium, kinetics, optimization and field studies, J. Environ. Chem. Eng. 2 (1) (2014) 46–55, doi:10.1016/j.jece.2013 .11.027.

[32] M. Ganesapillai, P. Simha, A. Zabaniotou, Closed-loop fertility cycle: realizing sustainability in sanitation and agricultural production through the design and implementation of nutrient recovery systems for human urine, Sustain. Prod. Consum. 4 (2015a) 36–46, doi:10.1016/j.spc .2015.08.004.

[33] M. Ganesapillai, P. Simha, The rationale for alternative fertilization: equilibrium isotherm, kinetics and mass transfer analysis for urea-nitrogen adsorption from cow urine, Resour. Efficient Technol. 1 (2) (2015b) 90–97, doi:10.1016/j.reffit.2015.11.001.

[34] G. Yan, T. Viraraghavan, Heavy metal removal in a biosorption column by immobilized *M. rouxii* biomass, Bioresour. Technol. 78 (3) (2001) 243–249, doi:10.1016/S0960-8524(01)00020-7.

[35] Z. Aksu, F. Gönen, Biosorption of phenol by immobilized activated sludge in a continuous packed bed, Prediction of breakthrough curves, Process Biochem. 39 (2004) 599–613, doi:10.1016/S0032-9592(03)00132-8.

[36] X.D. Liu, S. Tokura, M. Haruki, N. Nishi, N. Sakairi, Surface modification of nonporous glass beads with chitosan and their adsorption property for transition metal ions, Carbohydr. Poly. 49 (2) (2002) 103–108, doi:10.1016/S0144-8617(01)00308-3.

[37] J.M. Navarro, G. Durand, Modification of yeast metabolism by immobilization onto porous glass, Appl. Microbiol. Biotechnol. 4 (4) (1977) 243–254, doi:10.1007/BF00931261.

[38] M.C. Lu, J.N. Chen, K.T. Chang, Effect of adsorbents coated with titanium dioxide on the photocatalytic degradation of propoxur, Chemosphere 38 (3) (1999) 617–627, doi:10.1016/S0045 -6535(98)00204-5.

[39] X. Zhang, M. Zhou, L. Lei, Preparation of photocatalytic TiO_2 coatings of nanosized particles on activated carbon by AP-MOCVD, Carbon 43 (8) (2005) 1700–1708, doi:10.1016/j.carbon.2005.02.013.

[40] A.A. Ahmad, B.H. Hameed, Fixed-bed adsorption of reactive azo dye onto granular activated carbon prepared from waste, J. Hazard. Mater. 175 (2010) 298–303, doi:10.1016/j.jhazmat.2009.10.003.

[41] L. Monser, N. Adhoum, Modified activated carbon for the removal of copper, zinc, chromium and cyanide from wastewater, Sep. Purif. Technol. 26 (2–3) (2002) 137–146, doi:10.1016/S1383-5866(01)00155-1.

[42] H.G. Park, T.W. Kim, M.Y. Chae, I. Yoo, Activated carbon-containing alginate adsorbent for the simultaneous removal of heavy metals and toxic organics, Process Biochem. 42 (10) (2007) 1371–1377, doi:10.1016/ j.procbio.2007.06.016.

[43] A.P. Lim, A.Z. Aris, Continuo us fixed-bed column study and adsorption modeling: removal of cadmium (II) and lead (II) ions in aqueous solution by dead calcareous skeletons, Biochem. Eng. J. 87 (2014) 50–61, doi:10.1016/j.bej.2014.03.019.

[44] T.K. With, T.D. Petersen, B. Petersen, A simple spectrophotometric method for the determination of urea in blood and urine, J. Clin. Pathol. 14 (1961) 202–204.

[45] J. Goel, K. Kadirvelu, C. Rajagopal, V. Kumar Garg, Removal of lead(II) by adsorption using treated granular activated carbon: batch and column studies, J. Hazard. Mater. 125 (1–3) (2005) 211–220, doi:10.1016/j .jhazmat.2005.05.032.

[46] J.T. Yeh, H.W. Pennline, K.P. Resnik, Study of CO_2 absorption and desorption in a packed column, Energ. Fuel 15 (2) (2001) 274–278, doi:10.1021/ef0002389.

[47] Z. Aksu, F. Gönen, Z. Demircan, Biosorption of chromium (VI) ions by Mowital®B30H resin immobilized activated sludge in a packed bed: comparison with granular activated carbon, Process Biochem. 38 (2) (2002) 175–186, doi:10.1016/S0032-9592(02)00053-5.

[48] E. Malkoc, Y. Nuhoglu, M. Dundar, Adsorption of chromium(VI) on pomace – An olive oil industry waste: batch and column studies, J. Hazard. Mater. 138 (1) (2006) 142–151, doi:10.1016/j.jhazmat .2006.05.051.

[49] T.V.N. Padmesh, K. Vijayaraghavan, G. Sekaran, M. Velan, Batch and column studies on biosorption of acid dyes on fresh water macro alga

Azolla filiculoides, J. Hazard. Mater. 125 (1–3) (2005) 121–129, doi:10.1016/j.jhazmat.2005.05.014.

[50] B. Volesky, J. Weber, J.M. Park, Continuous-flow metal biosorption in a regenerable Sargassum column, Water Res. 37 (2) (2003) 297–306, doi:10.1016/S0043-1354(02)00282-8.

[51] K. Vijayaraghavan, J. Jegan, K. Palanivelu, M. Velan, Batch and column removal of copper from aqueous solution using a brown marine alga Turbinaria ornata, Chem. Eng. J. 106 (2) (2005) 177–184, doi:10.1016/j.cej.2004.12.039.

[52] T.S. Singh, K.K. Pant, Experimental and modelling studies on fixed bed adsorption of As(III) ions from aqueous solution, Sep. Purif. Technol. 48 (3) (2006) 288–296, doi:10.1016/j.seppur.2005.07.035.

[53] G.S. Bohart, E.Q. Adams, Some aspects of the behavior of charcoal with respect to chlorine, J. Am. Chem. Soc. 42 (3) (1920) 523–544, doi:10.1021/ja01448a018.

[54] H.C. Thomas, Heterogeneous ion exchange in a flowing system, J. Am. Chem. Soc. 66 (10) (1944) 1664–1666, doi:10.1021/ja01238a017.

[55] Y.H. Yoon, J.H. Nelson, Application of gas adsorption kinetics a theoretical model for respirator cartridge service life, Am. Ind. Hyg. Assoc. J. 45 (8) (1984) 509–516, doi:10.1080/15298668491400197.

[56] P. Simha, M. Mathew, M. Ganesapillai, Empirical modeling of drying kinetics and microwave assisted extraction of bioactive compounds from Adathoda vasica and Cymbopogon citratus, AEJ (2016) doi:10.1016/j.aej.2015.12.020.

[57] D.M. Kool, E. Hoffland, S. Abrahamse, J.W. van Groenigen, What artificial urine composition is adequate for simulating soil N_2O fluxes and mineral N dynamics?, Soil Biol. Biochem. 38 (7) (2006) 1757–1763, doi:10.1016/j.soilbio.2005.11.030.

[58] A. van Vuuren, M. Smits, Effect of nitrogen and sodium chloride intake on production and composition of urine in dairy cows, in: S.C. Jarvis, B.F. Pain (Eds.), Gaseous Nitrogen Emissions from Grasslands, CAB International, Okehampton, 1997.

[59] D.C.K. Ko, J.F. Porter, G. McKay, Optimised correlations for the fixed-bed adsorption of metal ions on bone char, Chem. Eng. Sci. 55 (23) (2000) 5819–5829, doi:10.1016/S0009-2509(00)00416-4.

[60] I.A.W. Tan, A.L. Ahmad, B.H. Hameed, Adsorption of basic dye using activated carbon prepared from oil palm shell: batch and fixed bed studies, Desalination 225 (1–3) (2008) 13–28, doi:10.1016/j.desal .2007.07.005.